

Article

Mercury Capture from Flue Gas Using Palladium Nanoparticle-Decorated Substrates as Injected Sorbent

Quentin J. Lineberry, Yan Cao, Yi Lin, Sayata Ghose, John W. Connell, and Wei-Ping Pan

Energy Fuels, **Article ASAP** • DOI: 10.1021/ef800733h • Publication Date (Web): 11 February 2009

Downloaded from <http://pubs.acs.org> on February 17, 2009

More About This Article

Additional resources and features associated with this article are available within the HTML version:

- Supporting Information
- Access to high resolution figures
- Links to articles and content related to this article
- Copyright permission to reproduce figures and/or text from this article

[View the Full Text HTML](#)



ACS Publications
High quality. High impact.

Energy & Fuels is published by the American Chemical Society, 1155 Sixteenth Street N.W., Washington, DC 20036

Mercury Capture from Flue Gas Using Palladium Nanoparticle-Decorated Substrates as Injected Sorbent

Quentin J. Lineberry,[†] Yan Cao,[†] Yi Lin,^{‡,§} Sayata Ghose,^{||} John W. Connell,[‡] and Wei-Ping Pan^{*,†}

Institute for Combustion Science and Environmental Technology (ICSET), Western Kentucky University, 2413 Nashville Road—STE C2, Bowling Green, Kentucky 42101, NASA Langley Research Center, Advanced Materials and Processing Branch, Mail Stop 226, Hampton, Virginia 23681, and National Institute of Aerospace, 100 Exploration Way, Hampton, Virginia 23666

Received August 31, 2008. Revised Manuscript Received January 9, 2009

Although the Clean Air Mercury Rule (CAMR) was recently vacated by the District of Columbia Court of Appeals, efficient mercury (Hg) capture is still an important topic for the coal-fired power plant industry. Several states have Hg emission regulations that are even more stringent than CAMR guidelines. All coals contain Hg, which is released during combustion. Significant research efforts have been made to capture this toxic element before it is released to the atmosphere where it can stay suspended and travel for great distances. A variety of approaches have been examined, among which the injection of sorbent materials such as powdered activated carbon (PAC) is the current method of choice. The work presented here examined the mercury capture capability of various carbon substrates decorated with metal nanoparticles when injected as sorbents. Sorbent injections were carried out in a Hg in air mixture for laboratory-scale screening and in a real flue gas at a coal-fired power plant. It was found that palladium-decorated carbon substrates showed excellent mercury capture capabilities, with total efficiencies greater than 90% in laboratory-scale tests. In the real flue gas, the total efficiency was on the order of ~60%, comparable to the benchmark commercial sorbent Darco Hg-LH, a brominated PAC, although the tested adsorbents had much lower surface areas. The results of this study are presented herein. Novel mercury capture from a coal-fired flue gas was achieved using carbon substrates decorated with palladium nanoparticles.

Introduction

Federal level mercury emission regulations are currently in an unknown state because of the U.S. Court of Appeals for the District of Columbia vacating the Clean Air Mercury Rule (CAMR).¹ However, several states have enacted Hg emission regulations that are more stringent than the CAMR milestones. For example, Massachusetts will require power plants to achieve 95% removal efficiency or an emission standard of 0.0025 lbs/GW h by 2012, while Maryland will require 90% removal efficiency by 2013.^{2,3} Delaware will also require a removal efficiency of 90% by 2013.⁴ To ensure compliance with these regulations, as well as future federal regulation, coal-fired power plants need to know their current emission levels. With this knowledge, decisions regarding the implementation of various air pollution control devices (APCDs) to control Hg, as well as their intended targets, will be made. APCDs include cold-side and hot-side electrostatic precipitators (CS-ESPs and HS-ESPs), baghouses/Fabric Filters (FF), wet flue gas desulfurization units (WFGDs), and selective catalytic reduction systems (SCRs),

which are intended for control of particulate matter (PM), sulfur dioxide (SO_x), and nitrogen oxides (NO_x), respectively. All of these APCDs have co-benefits for Hg capture but not always at the desired level. To gain additional Hg capture efficiency, other alternatives for Hg control have been demonstrated. For example, the injection of sorbent materials, in conjunction with the aforementioned APCDs, is a leading mercury control technology.⁵ Some of the most widely used adsorbents are powdered activated carbons (PACs), which are modified to enhance the affinity of their surfaces to Hg. Activated carbon injection (ACI) is used to convert gaseous mercury into activated carbon-bound mercury which will be subsequently captured in an ESP or baghouse as particulate bound mercury (Hg(P)).⁵

The total mercury in flue gas (Hg(T)) occurs primarily in three forms: elemental mercury represented by the symbol Hg⁰, oxidized mercury represented by the symbol Hg²⁺, and particulate-bound mercury represented by the symbol Hg(P).⁶ Mercury is released from coal primarily as Hg⁰. As the flue gas cools in the downstream ductwork of the boiler, some of the Hg⁰ can be oxidized to Hg²⁺. The degree of oxidation is affected by the temperature of the flue gas and its rate of change, as well as the other species present in the gas. The species present in the flue gas can be a result of the species present in the coal before combustion, such as Cl- or S-based compounds, or they can originate from injection into the flue gas stream,

* To whom correspondence should be addressed. E-mail: wei-ping.pan@wku.edu. Phone: (270)745-2272. Fax: (270)745-2221.

[†] Western Kentucky University.

[‡] NASA Langley Research Center.

[§] NASA Postdoctoral Program Fellow.

^{||} National Institute of Aerospace.

(1) (a) Hogue, C. Mercury Rule Overturned. *Chem. Eng. News* **2008**, 6. (b) State of New Jersey, et al v. EPA, F.3d, Docket No. 05–1097 (D.C. Circuit, Feb. 8, 2008).

(2) Code of Massachusetts Regulations. 310 CMR 7.29(5)(a)3.e (2006).

(3) COMAR 26.11.27.04.D (2006).

(4) Delaware Regulation No. 1146, 6.0 (2006).

(5) Pavlish, J. H.; et al. Status review of mercury control options for coal-fired power plants. *Fuel Process. Technol.* **2003**, 82, 89–165.

(6) Galbreath, K.; Zygarlicke, C. Mercury Speciation in Coal Combustion and Gasification Flue Gases. *Environ. Sci. Technol.* **1996**, 30, 2421–2426.

such as NH_3 for SCR performance. While some species, such as HCl and HBr , can promote the oxidation of elemental mercury, other species, such as NH_3 , have no effect.^{7,8}

Hg^{2+} and Hg(P) are more easily captured by existing APCDs than elemental mercury.⁹ However, there are species in the flue gas that can interfere/compete with mercury adsorption on activated carbon, such as SO_2 and SO_3 .¹⁰ Therefore, while an activated carbon may perform well in laboratory experiments that do not contain these species in the simulated flue gas, its performance at a power plant is likely to be reduced because of these inhibiting species.

In recent years, there has been an increasing interest in the use of metals and metal oxides to oxidize or capture Hg. For example, Granite and his co-workers examined several metals for their possible use as sorbents to capture Hg from gasification fuel gases at elevated temperatures.¹¹ Among these metals, Pd appeared to be the best candidate by capturing 54% of the Hg from a simulated fuel gas at 288 °C.¹¹ Poulston and his co-workers studied platinum and palladium elements (Pt and Pd) supported on alumina. While both metals were able to capture Hg, once again, Pd was a better sorbent. On the basis of X-ray diffraction (XRD) experiments following Hg exposure, there was evidence for the presence of a Hg in Pd solid solution.¹²

The goal of this work was to determine if Pd nanoparticle-decorated carbon substrates could be used as an adsorbent for the effective capture of mercury in a coal-fired power plant. Substrates used included single-walled carbon nanotubes (SWNTs), graphite, carbonized chicken litter, activated carbon from carbonized chicken litter, and ash from a coal-fired power plant. The metallic particles, randomly dispersed on these substrates, are typically relatively small (100 nm or less) and consequently provide a relatively large surface area/volume.

Experimental Section

Materials Selection. Purified HiPco SWNTs (lot P0325) were purchased from Carbon Nanotechnologies, Inc. and used as-received. Expanded graphite (grade 3775, lot 3438) was donated by Asbury Carbons, Inc. Palladium (II) acetate, $\text{Pd}(\text{C}_2\text{H}_3\text{O}_2)_2$, was purchased from Sigma-Aldrich.

In addition to SWNTs and expanded graphite, three other materials were also modified with palladium—carbonized chicken litter, activated carbon from chicken litter, and ash from a selected power plant. The preparation of the carbonized chicken litter and activated carbon from chicken litter can be found elsewhere.¹³

Sample Preparation. The method used for metal deposition onto the substrates was based upon a procedure published in a patent

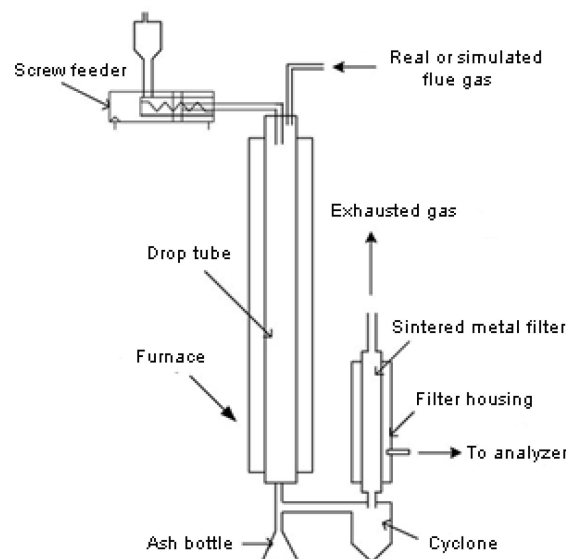


Figure 1. Schematic of the drop-tube reactor used for the mercury capture tests.

application.¹⁴ The procedure involves physically mixing a metal salt with the substrate, followed by thermal reduction of the salt to deposit metal nanoparticles on the surface of the substrate. In brief, the substrate is mixed with the appropriate metal acetate and subsequently heated in an inert atmosphere to 350 °C and held for 3 h in a horizontal stainless steel tube furnace. The stainless steel tubing was setup to allow purging with Ultra High Purity Nitrogen (UHP N_2) gas. The samples were mixed in a mortar and pestle and transferred to a test tube. The loaded test tube was placed in the stainless steel tube, which was placed in the furnace. The setup was allowed to purge for 30 min with UHP N_2 , at which time, the temperature program was started. The samples were allowed to cool to room temperature under flowing nitrogen. Samples with various metal concentrations were prepared, including 2, 10, and 20% by weight. The calculation was based on the theoretically full conversion of the metal acetate into the corresponding metal.

Characterization. High Resolution Scanning Electron Microscopy (HRSEM) experiments were conducted on a Hitachi S-5200 field emission scanning electron microscope. The microscope was operated between 5–25 kV. To prepare the samples for examination, silver paste was applied to an SEM stub. The samples were then sprinkled onto the paste. The stubs were then placed into an oven at ~90 °C overnight to allow the paste to dry.

XRD experiments were carried out on a Thermo ARL X'TRA X-ray diffractometer using $\text{Cu K}\alpha$ radiation and a peltier-cooled detector. The configuration of the instrument was $\theta:\theta$. The scan rate was 0.1–2.5 °/min. The powdered samples were packed into quartz sample holders. The International Centre for Diffraction Data (ICDD) Powder Diffraction File, PDF-4+, was the database used for phase identification.

The Brunauer–Emmett–Teller surface area of the samples was determined using a Micromeritics ASAP 2020 surface area and porosity analyzer with silica–alumina as the standard and nitrogen as the adsorbate. The sample sizes varied depending on the surface area of the material being tested.

Mercury Capture Testing. Mercury capture testing was performed using a laboratory-scale drop-tube reactor, as shown in Figure 1. This setup was used for both laboratory testing with Hg in air and for onsite testing with real flue gas without any modifications except for the sample gas being introduced to the system. The laboratory testing was done to show that the palladium

(7) Cao, Y.; Gao, Z.; Zhu, J.; Wang, Q.; Huang, Y.; Chiu, C.; Parker, B.; Chu, P.; Pan, W. P. Impacts of Halogen Additions on Mercury Oxidation, in A Slipstream Selective Catalyst Reduction (SCR), Reactor When Burning Sub-Bituminous Coal. *Environ. Sci. Technol.* **2008**, *42*, 256–261.

(8) Cao, Y.; Chen, B.; Wu, J.; Cui, H.; Smith, J.; Chen, C.-K.; Chu, P.; Pan, W.-P. Study of Mercury Oxidation by a Selective Catalytic Reduction Catalyst in a Pilot-Scale Slipstream Reactor at a Utility Boiler Burning Bituminous Coal. *Energy Fuels* **2007**, *21*, 145–156.

(9) Presto, A. A.; Granite, E. J. Survey of Catalysts for Oxidation of Mercury in Flue Gas. *Environ. Sci. Technol.* **2006**, *40* (18), 5601–5609.

(10) Presto, A. A.; Granite, E. J. Impact of Sulfur Oxides on Mercury Capture by Activated Carbon. *Environ. Sci. Technol.* **2007**, *41* (18), 6579–6584.

(11) Granite, E. J.; Myers, C. R.; King, W. P.; Stanko, D. C.; Pennline, H. W. Sorbents for Mercury Capture from Fuel Gas with Application to Gasification. *Ind. Eng. Chem. Res.* **2006**, *45*, 4844–4848.

(12) Poulston, S.; Granite, E. J.; Pennline, H. W.; Myers, C. R.; Stanko, D. P.; Hamilton, H.; Rowsell, L.; Smith, A. W. J.; Ilkenhans, T.; Chu, W. Metal sorbents for high temperature mercury capture from fuel gas. *Fuel* **2007**, *86*, 2201–2203.

(13) Cui, H.; Cao, Y.; Pan, W. P. Preparation of activated carbon for mercury capture from chicken waste and coal. *J. Anal. Appl. Pyrolysis* **2007**, *80* (2), 319–324.

(14) Watson, K. A.; Fallbach, M. J.; Ghose, S.; Smith, J. G., Jr.; Delozier, D. M.; Connell, J. W. U.S. Provisional Application No. 60/780,173 filed on March 6, 2006 for “Method of Depositing Metals Onto Carbon Allotropes and Compositions Therefrom”.

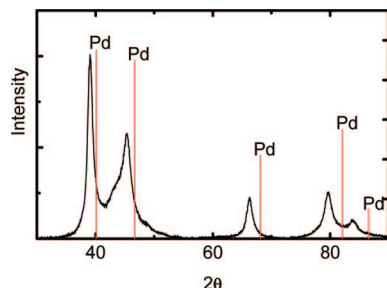


Figure 2. XRD pattern of SWNT with 10% Pd overlaid with ICDD PDF card for Pd (#00-046-1043).

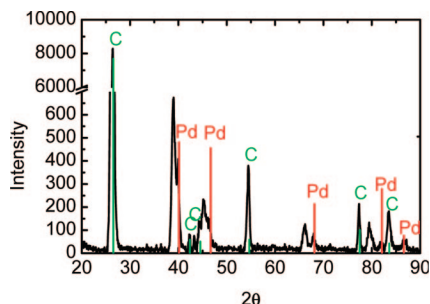


Figure 3. XRD pattern of graphite with 10% Pd overlaid with ICDD cards for graphite (#00-056-0159) and Pd (#00-046-0143).

Table 1. Positions of Pd (111) Peaks for Samples Tested

sample substrate	Pd Content (wt %)	Pd(111) 2θ values (deg)
palladium	100	40.1
SWNT	10	39.08
activated carbon from chicken litter	10	39.00
carbonized chicken litter	2	39.32
carbonized chicken litter	10	39.06
carbonized chicken litter	20	39.04
ash	10	39.28
graphite	10	38.98
graphite	20	39.30

decorated substrates could capture mercury. The onsite testing was done to see how the adsorbents performed in an actual flue gas with its various interfering species. For onsite testing, a power plant burning a sub-bituminous coal was used. The Powder River Basin (PRB) coal burned at the plant had a low chlorine content (85–125 ppm); such a low chlorine content has been shown to produce a flue gas at the ESP inlet that contains mostly elemental mercury. For laboratory-scale testing, a PS Analytical mercury vapor generator was used to introduce Hg into an air stream at a concentration of 10,000–13,000 ng/Nm³.

The main portion of the reactor consisted of a 2" ID stainless steel pipe that was previously verified to be inert to mercury transformation. The reactor was heated to ~150 °C by an electric furnace to simulate and maintain the temperature at the ESP inlet. For onsite testing, the flue gas was extracted just prior to the ESP inlet and was reintroduced just downstream of the extraction point but still prior to the ESP inlet.

Hg in air (laboratory testing) or real flue gas (onsite testing) entered the reactor from the top and passed through the reactor, cyclone, and inertial filter, where the gas was extracted and delivered to the mercury measurement system. The purpose of the cyclone and inertial filter was to remove the ash to prevent introduction of a bias brought on by the interference between the ash and the mercury during the measurement process. The adsorbent was mixed with ash to allow for controlled feeding of the adsorbent since the screw feeder used would have introduced excessive amounts of the adsorbent at its lowest setting without the ash dilution. Since PRB ash had poor flow characteristics from the feeder, the dilution ash used was from a bituminous coal. The adsorbent was introduced from the top of the reactor via a screw feeder at a rate of 4 pounds per million actual cubic feet (lb/MMacf). The residence time of

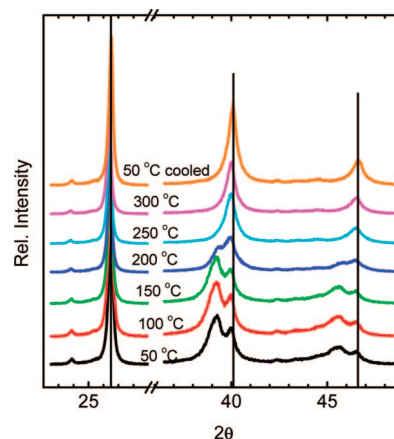


Figure 4. Shift/consolidation of Pd peaks as a function of temperature. Diffractograms were taken every 50 °C up to 300 °C and again after cooling to 50 °C. The vertical lines represent Pd PDF lines.

the adsorbent in the reactor was approximately one second (1 s) for both testing scenarios.

The mercury concentration was determined using a PS Analytical semi-continuous emission monitor (SCEM), with the sample being extracted from the inertial filter section to prevent ash interference.

Results and Discussion

Modification of Substrates. XRD was used to determine the state of the palladium on the substrates—elemental, palladium (II) acetate, or palladium oxide. The XRD spectra of all of the samples examined, including SWNT, carbonized chicken litter, and activated carbon from chicken litter, showed the typical Pd(0) pattern, that is, evidence for the presence of elemental palladium. For example, the XRD pattern of the SWNT with 10% Pd sample seemed to be quite typical for bulk Pd metal (PDF card #00-046-1043), as shown in Figure 2.

Interestingly, all peaks corresponding to Pd(0) in the above sample (and also for carbonized chicken litter and activated carbon from chicken litter samples) were systematically downshifted to lower 2θ angle (or higher *d*-spacing) from those of bulk Pd metal. For example, the (111) and (200) reflections for Pd(0) in the XRD pattern of the SWNT with 10% Pd sample appear at 39.1° and 45.4°, respectively, much lower than the standard PDF card (40.1° and 46.7°).

This phenomenon of peak-shift was even more intriguing for some other samples, although, perhaps a result of the same mechanism. In the XRD pattern of the graphite with 10% Pd sample (Figure 3), while there are prominent diffraction peaks corresponding to graphite (26.5° in particular), the (111) reflection of elemental Pd is also present but appears as a doublet with the two peak values both at somewhat lower 2θ angles (40.1° and 39.0°) than the singlet in the standard pattern.

In fact, the XRD spectra of most of the Pd nanoparticle-decorated samples showed either downshifted-2θ peaks (SWNT, carbonized chicken litter, and activated carbon from chicken litter samples) or doublets (expanded graphite and ash samples) ((111) peaks summarized in Table 1). These observations might share similar mechanistic origins, which could be from one or both of the following two possibilities. First, it could be a result of a uniform strain, most likely thermal, imparted to the Pd nanocrystals as they were deposited onto the substrates resulting in a unit cell somewhat larger than expected. Alternatively, it could be a result of oxygen or carbon inclusion into the Pd

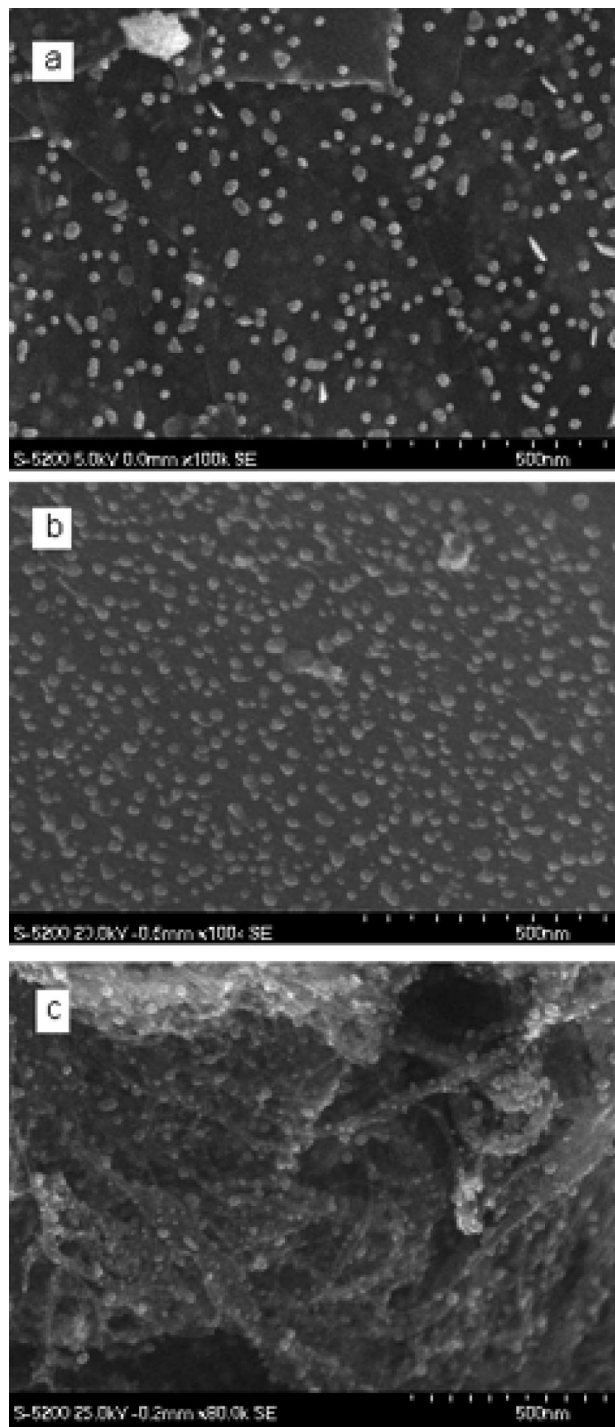


Figure 5. HRSEM images of (a) graphite with 10% Pd, (b) carbonized chicken litter with 10% Pd, and (c) SWNT with 10% Pd.

crystal lattice as suggested by the literature.¹⁵ In the SWNT with 10% Pd sample, for example, such a shift may correspond to a rather uniform increase of the Pd unit cell of 2.5%.

In-situ high temperature XRD experiments were conducted to further study the cause of the XRD pattern shift. Figure 4 shows the results of heating a graphite with 20% Pd sample to 300 °C with diffraction patterns collected every 50 °C and a final pattern taken after the specimen was cooled to 50 °C. While

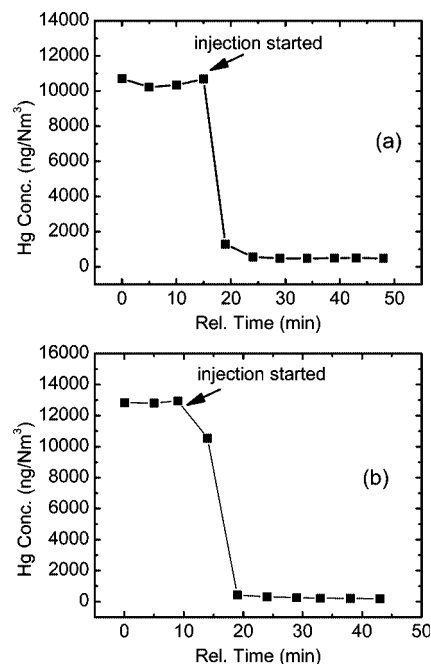


Figure 6. Laboratory-scale total mercury capture results for (a) SWNT with 10% Pd and (b) graphite with 10% Pd (adsorbent injection rate = 4 lb/MMacf).

Table 2. Average Composition of Flue Gas at Power Plant during Testing

species	average amount
Hg	10.8 $\mu\text{g}/\text{Nm}^3$
Hg(0)/Hg(T)	0.67
SO _x	250 ppm
NO _x	75 ppm
HCl	5 ppm
moisture	14%

the position and shape of the reference peak at 26.5° for graphite hardly changed, it is apparent that the doublet just below 40° gradually coalesced into a single peak at a higher angle (~40.1°) when the reaction temperature was raised from 50 to 300 °C. This result seems to indicate that the origin of the doublet formation or the peak downshift is more likely due to the first possibility listed above, namely the thermal stress imparted to the crystallized Pd nanoparticles during the process of growth/decoration onto the carbon substrates. In addition, it seems that slower heating rates or extended isothermal holds could produce Pd nanoparticles with crystalline constants more similar to bulk elemental Pd, while rapid heating rates or no isothermal holds result in less homogeneous thermal stress. In the circumstances of the latter, two Pd(0) phases of slightly different unit cell parameters formed, thus showing doublets in the XRD spectrum, with the phase with lower diffraction angles experiencing stronger thermal stress.

The Pd metals from thermal decomposition of palladium (II) acetate in its mixture with different carbon substrates are in the form of nanoparticles. Figure 5a shows a typical HRSEM image obtained for graphite with 10% Pd. The light colored spots are attributed to Pd, while the darker background and features are a result of the graphite surface. From Figure 5a, it can be seen that the Pd particles distribute relatively evenly over the substrates and with particle sizes typically less than 50 nm for all samples examined (averaged 19 nm). The distribution of the Pd nanoparticles is largely homogeneous. In addition, increasing the concentration of the Pd with respect to the substrate resulted in a slight increase to the average size of the Pd nanoparticles

(15) Ferhat-Hamida, Z.; Barbier, J.; Labruquere, S.; Duprez, D. The chemical state of palladium in alkene and acetylene oxidation: A study by XRD, electron microscopy and TG-DTG analysis. *Appl. Catal., B* **2001**, 29, 195–205.

Table 3. Tabular Onsite Hg Capture Data and Surface Areas for Tested Samples

injected substrate ^a	Pd content (wt %)	Hg(T) baseline concentration (ng/Nm ³) ^b	Hg(0) baseline concentration (ng/Nm ³) ^b	Hg(T) capture eff. (%)	Hg(0) capture eff. (%)	surface area (m ² /g)
dilution ash (control)		10428	6851	13.83%	12.49%	N/A
Darco Hg-LH		11335	7340	58.49%	64.48%	540
Darco Hg-LH		10418	7047	53.07%	61.75%	540
activated carbon from chicken litter				28.43%	23.75%	4.8
activated carbon from chicken litter	10	11660	7507	59.89%	49.53%	4.9
ash				12.26%	14.86%	15
ash	10	11651	7448	55.43%	62.18%	13
graphite				7.60%	7.99%	22
graphite	2	10806	7100	45.90%	46.13%	21
graphite	10	10017	7504	57.33%	63.55%	23
graphite	20	10780	7094	60.07%	73.07%	23
carbonized chicken litter				17.91%	13.44%	4.7
carbonized chicken litter	2	10275	7074	60.73%	62.94%	9.6
carbonized chicken litter	10	10754	7036	59.21%	54.64%	9.3
carbonized chicken litter	20	10237	6927	62.20%	63.03%	8.6

^a Adsorbent injection rate = 4 lb/MMacf. ^b O₂ corrected [Hg] = [Hg] × (20.9 – 3)/(20.9 – [O₂]).

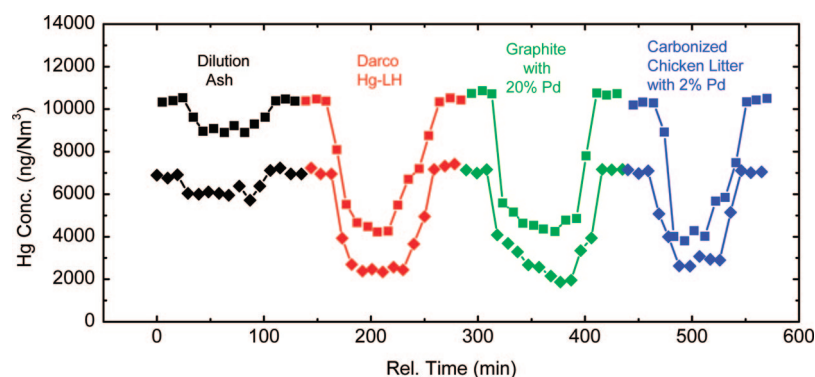


Figure 7. Onsite mercury capture data for selected samples with an adsorbent injection rate of 4 lb/MMacf (squares represent Hg(T) and diamonds represent Hg(0)).

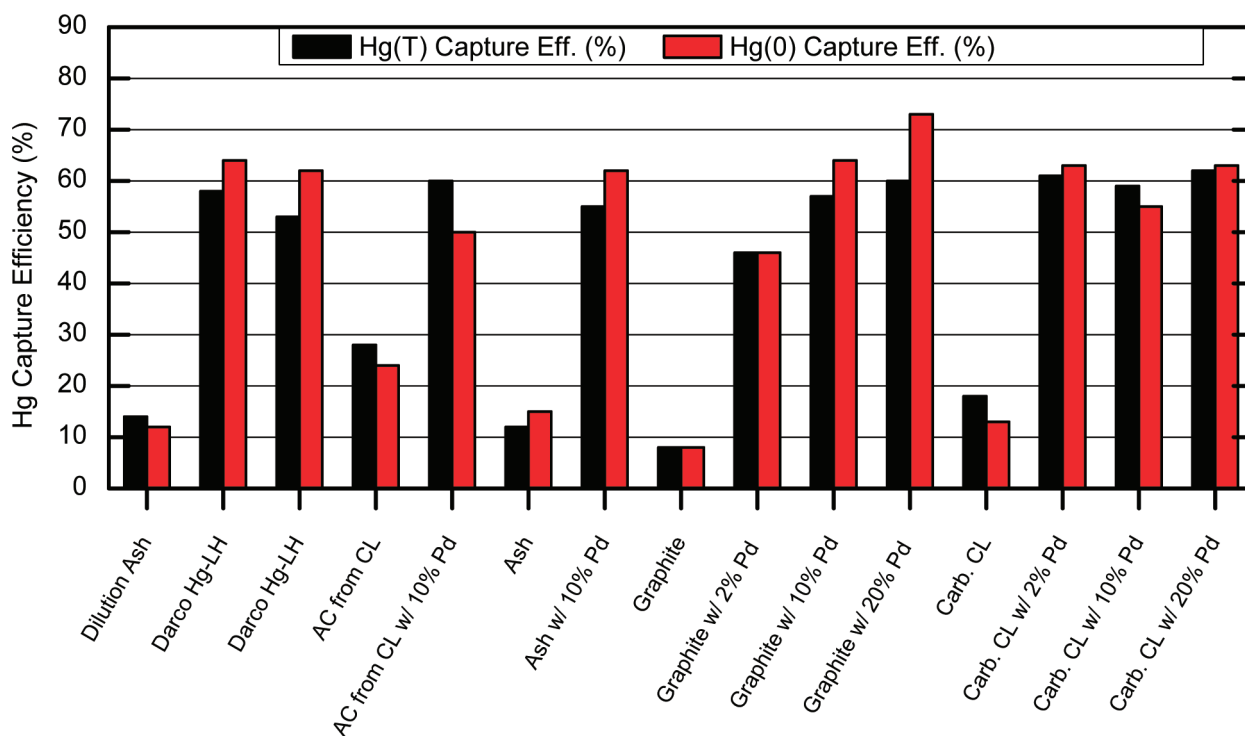


Figure 8. Histogram showing levels of total and elemental mercury capture from onsite testing for all samples tested.

(e.g., average size of 24 nm for 20% Pd on graphite) with a marked increase in their surface-distribution density.

The microscopy results for other carbon substrates were similar, with observed Pd nanoparticles of somewhat different

sizes and size distributions. The HRSEM images of carbonized chicken litter and SWNTs, both with 10% Pd, are shown in panels b and c of Figure 5, respectively. The average size for these samples was calculated to be 21 nm.

Laboratory-Scale Mercury Capture Tests. Mercury capture tests were performed in the laboratory using the reactor depicted in Figure 1. A gas mixture consisting of $\sim 11,000$ ng/Nm³ Hg in air was obtained by introducing gaseous elemental mercury produced using a PS Analytical mercury vapor generator into an air stream. This gas then passed through the system, and the Hg sample was extracted from the inertial filter.

Figure 6 shows the mercury capture data for SWNT and graphite samples both with 10% Pd. Immediately upon injection of the adsorbents, there was a significant decrease of detectable Hg concentration. Overall, the injection of the SWNT with 10% Pd sample resulted in a decrease of 95.4% of the total Hg, while injection of graphite with 10% Pd resulted in a decrease of 98.2% of the total Hg concentration introduced to the system.

The promising laboratory-scale results obtained warranted the study of these materials onsite using real flue gas to investigate how the interfering species affect the Hg capture efficiency.

Onsite Mercury Capture Tests. Measuring the mercury capture capabilities of adsorbents in a power plant is the ultimate benchmark for determining their real-world effectiveness. When doing laboratory-scale testing, the complications introduced from the complexity of the real flue gas are reduced or eliminated allowing the true efficiency of the material toward Hg capture alone to be determined. Other species in real flue gas, such as SO₂, compete for the same active sites on the adsorbent as Hg, thus, making interpretation of the capture data more complicated.

Hg capture efficiency was calculated using the average baseline mercury concentration, [Hg]_{baseline}, and the average mercury concentration during sorbent injection, [Hg]_{sorbent} according to

$$\text{Capture Eff.} = \{([Hg]_{\text{baseline}} - [Hg]_{\text{sorbent}})/[Hg]_{\text{baseline}}\} \times 100\% \quad (1)$$

Onsite mercury capture tests were performed on the same small-scale drop tube furnace used in the laboratory-scale tests. The only difference was that, for the onsite testing, real flue gas from a utility power plant that burns a sub-bituminous coal (PRB) was used over multiple test periods. Table 2 lists the

typical composition of the flue gas during the testing periods. To facilitate controlled addition of the adsorbents to the flue gas using the screw feeder, the adsorbents were mixed with a bituminous ash sample to lower the feed rate of the adsorbent material.

Table 3 and Figures 7 and 8 show the Hg capture data for the various samples tested. While typical capture efficiencies for the unmodified substrates investigated were mostly far below 30%, the decoration of Pd nanoparticles onto the substrates resulted in a marked increase in Hg capture capability on the order of 45% or more. In fact, except for that of graphite with 2% Pd sample, the capture efficiencies (both Hg(T) and Hg(0)) for all other Pd nanoparticle-decorated carbon samples tested were comparable to or even better than Darco Hg-LH (capture efficiency 58.5% with the dilution ash accounting for $\sim 13\%$). In addition, it appears that higher loading levels promoted Hg capture, despite the somewhat increased Pd nanoparticle size according to SEM images.

The enhanced capture of Hg from flue gas by these novel materials is not unexpected, since Pd metal is known to provide efficient Hg adsorption as discussed previously.¹¹ For example, Pd was shown to catalyze oxidation of mercury in a fixed-bed (instead of as injected sorbent as shown here), which allows the pollutant to be more easily captured using existing APCDs.⁹ In this work, the highly dispersed Pd nanoparticles with large accessible surface area could also be acting as an effective catalyst to promote the oxidation of Hg, resulting in the enhancement of Hg capture efficiency. The formation of a Pd–Hg alloy on the carbon substrate surface, also discussed in the literature, could contribute to the observed capture enhancement as well.¹²

Acknowledgment. This study was supported by the NASA GSRP through Grant NGT1–03012. Y.L. was supported by an appointment to the NASA Postdoctoral Program at the Langley Research Center, administered by Oak Ridge Associated Universities through NASA contract NNH06CC03B.

EF800733H